Characterization of Mycobacterium tuberculosis Mycolic Acids by Multiple-Stage Linear Ion-Trap Mass Spectrometry

Frankfater, Cheryl; Fujiwara, Hideji; Williams, Spencer J; Minnaard, Adriaan; Hsu, Fong-Fu

Published in:
Journal of the American Society for Mass Spectrometry

DOI:
10.1021/jasms.1c00310

Publication date:
2022

ACS Partner Journal

Journal of the American Society for Mass Spectrometry

pubs.acs.org/jasms

Research Article

Characterization of *Mycobacterium tuberculosis* Mycolic Acids by Multiple-Stage Linear Ion-Trap Mass Spectrometry

Cheryl Frankfater, Hideji Fujiwara, Spencer J. Williams, Adriaan Minnaard, and Fong-Fu Hsu*

Cite This: *J. Am. Soc. Mass Spectrom.* 2022, 33, 149−159

Read Online

ACCESS | Metrics & More | Article Recommendations | Supporting Information

ABSTRACT: *Mycobacterium tuberculosis* (Mtb) cells are known to synthesize very long chain (C60−90) structurally complex mycolic acids with various functional groups. In this study, we applied linear ion-trap (LIT) multiple-stage mass spectrometry (MS^n), combined with high-resolution mass spectrometry to study the mechanisms underlying the fragmentation processes of mycolic acid standards desorbed as lithiated adduct ions by ESI. This is followed by structural characterization of a Mtb mycolic acid family (Bovine strain). Using the insight fragmentation processes gained from the study, we are able to achieve a near complete characterization of the whole mycolic acid family, revealing the identity of the α-alkyl chain, the location of the functional groups including methyl, methoxy, and keto groups along the meroaldehyde chain in each lipid species. This study showcased the power of LIT MS^n toward structural determination of complex lipids in a mixture, which would be otherwise very difficult to define using other analytical techniques.

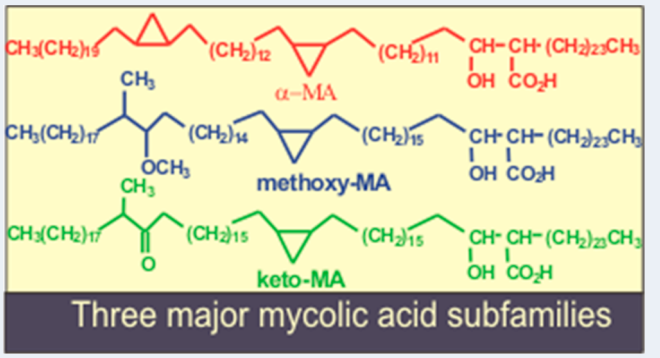

KEYWORDS: *linear ion trap mass spectrometry, high resolution mass spectrometry, cell envelope lipids, mycolic acids, Mycobacterium tuberculosis*

INTRODUCTION

Mycolic acids (MAs) are α-alkyl, β-hydroxy long-chain fatty acids (FAs). They are the major and specific lipid components in the mycobacterial cell envelope and play a crucial role in the cell wall architecture and impermeability that provide natural resistance of mycobacteria to most antibiotics for their survival and partake in mycobacterial pathogenicity.[1] Mycolic acids synthesized in *Mycobacteria* involve at least two discrete elongation systems, fatty acid synthase-I (FAS-I) and fatty acid synthase-II (FAS-II). The mycobacterial FAS II elongates medium-chain-length fatty acids previously synthesized by FAS I, leading to meromycolic acids, which are finally assembled to mycolic acids by Claisen-type condensation pathways to corporate acyl chain of Acyl-S-CoA derived from FAS-I.[2−4]

Mycobacterium tuberculosis (*M. tuberculosis*) (*Mtb*) is known to synthesize α-, methoxy-, and keto-mycolic acids. These mycolic acids consist of a C60−90 chain,[4] and the chain length and the abundances are dependent on the growth condition (e.g., growth rate), and the strain of the mycobacteria.[5,6] For example, the chain length of MA in *M. smegmatis* is significantly shorter than that in *Mtb* H37Rv, and a new bacterial *Segniliparus* genus is known to synthesize mycolic acids with chain length up to C100.[7,8]

Structural analysis of MA was started with a variety of techniques including IR, proton and carbon NMR, electron-impact MS, pyrolytic GC, as well as basic chemical analysis methods.[9,10] Finer structural detail was later achieved by the more advanced analytical techniques including GC/MS, electrospray (ESI) LC/MS, MALDI-MS, and FAB-tandem MS-MS[11−19] that allowed mycolate structures to be defined. However, none of the above mass spectrometric approaches offered a direct method to achieve complete structural characterization of the molecules.

We previously described a tandem mass spectrometric method to characterize fatty acid as lithiated ion desorbed by electrospray ionization (ESI).[20] We also applied linear ion-trap (LIT) multiple-stage mass spectrometry (MS^n) for complete characterization of the complex microbial lipid structures.[21−26] In this study, we will describe the ESI LIT MS^n approach toward complete structural characterization of the major *Mtb* mycolic acids as lithiated ions, revealing the location of functional groups on the meromycolic (meroaldehyde) chain and the identity of the α-alkyl group of the molecules.

Received: October 10, 2021
Revised: November 15, 2021
Accepted: November 16, 2021
Published: November 29, 2021

Scheme 1. Designation of (a) C54:2(20,14,13)/C26:0-αMA, (b) C60:2(18,18,17)/C26:0-kMA, and (c) C61:1(18,18,17)/26:0-mMA

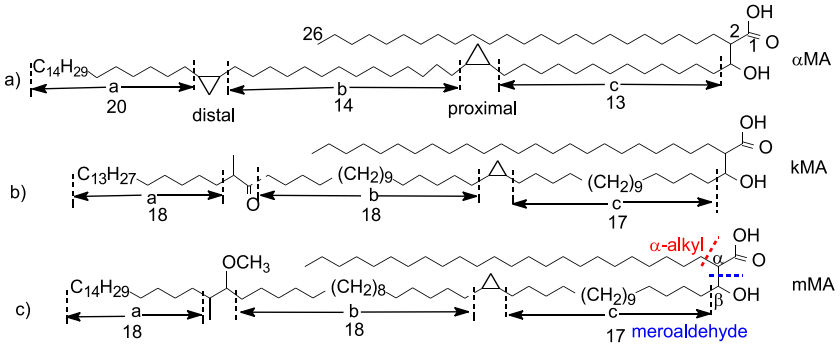

MATERIALS AND METHODS

Materials. C80 α-mycolic and C86 keto-mycolic acids were purchased from Avanti Polar Lipids Co. (Alabaster, AL, U.S.A.). Corynemycolic acid[27] and C80 methoxy-mycolic acid[28] were synthesized as described previously. *Mtb* mycolic acid (bovine strain) and all other solvents (spectroscopic grade) and chemicals (ACS grade) were obtained from Sigma Chemical Co. (St. Louis, MO).

Mass Spectrometry. Both high-resolution (R = 100 000 at m/z 400) and low-energy CID tandem mass spectrometric experiments were conducted on a Thermo Scientific (San Jose, CA) LTQ Orbitrap Velos mass spectrometer (MS) with Xcalibur operating system. Samples in methanol (around 50 pmol/μL) with 2 nmol/μL ^{7}LiOH were infused at 3 μL/min into the ESI source where the skimmer was set at ground potential, the electrospray needle was set at 4.0 kV, and the temperature of the heated capillary was 300 °C. The automatic gain control of the ion trap was set to 5×10^4 with a maximum injection time of 400 ms. Helium was used as the buffer and collision gas at a pressure of 1×10^{-3} mbar (0.75 mTorr). The MS^n experiments were carried out with an optimized relative collision energy ranging from 45 to 65% and with an activation q value at 0.25. The activation time was set for 10 ms to leave a minimal residual abundance of precursor ion (around 20%). The mass selection window for the precursor ions was set at 1 Da wide to admit the monoisotopic peak to the ion-trap for collision-induced dissociation (CID) for unit resolution detection in the ion-trap or high-resolution accurate mass detection in the Orbitrap mass analyzer. Mass spectra were accumulated in profile mode, typically for 5−20 min for MS^n spectra (n = 2,3,4).

Nomenclature. Very long chain *Mtb* mycolic acids are known to contain a meroaldehyde chain with cyclopropyl, methyl, keto, and methoxy branch. The heterogeneity of the meroaldehyde chain is derived from the variation of the chain length between the branches (functional groups). To facilitate data interpretation, we adopt the abbreviation previously used to define the structure.[1] The functional group (cyclopropyl, keto, or methyl branch) farthest away from the aldehyde end on the meroaldehyde chain is called distal functional group. The carbon number from the nonpolar ω-end to the distal functional group of the meroaldehyde chain is designated as **a**, the carbon number between the two functional groups is referred to as **b**, and the carbon number between the proximal functional group (normally a cyclopropane) to the β-hydroxy group mycolic acid is designated as **c** (c-chain). Thus, for example, the **a**, **b**, and **c**, for C80 α-mycolic acid with (2R)-2-[(1R)-1-Hydroxy-14-{2-[14-(2-eicosylcyclopropyl)tetradecyl]-cyclopropyl}tetradecyl]hexacosanoic acid structure, are 20, 14, and 13, respectively (Scheme 1). The designation of mycolic acid is in the form of mero/α-alkyl-MA as described previously.[29] Hence, the above-mentioned C80 α-mycolic acid is designated as C54:2(20,14,13)/C26:0-α-MA to reflect that the meroaldehyde contains a C54 chain with two unsaturation (cyclic bond), and a 24:0-α-alkyl chain (a 26:0-FA). The keto- and methoxy-MA are abbreviated as k-MA and m-MA, respectively. There is no distinction in the mass spectrometry of *cis*- or *trans*-mycolic acid, and thus the stereo specificity is not defined.

RESULTS AND DISCUSSION

Ion Formation of Mycolic Acids by ESI in the Negative Ion Mode. When subjected to ESI, MA, for example, Mtb MA readily formed $[M - H]^-$ ions (Figure s1a), and in the presence of Cl^-, low abundant $[M + Cl]^-$ ions can also be formed. The $[M + Cl]^-$ ions are labile and readily give rise to the $[M - H]^-$ ions by loss of HCl. MS^2 on the $[M -$

Table 1. HR Mass Measurement of *Mtb* Mycolic Acids (Bovine Strain) Detected as $[M - H + 2Li]^+$ Ions by ESI and the Ion Structures Deduced by LIT MS^n[a,b]

Table 1. HR mass measurement of *Mtb* mycolic acids (Bovine strain) detected as $[M - H + 2Li]^+$ ions by ESI and the ion structures deduced by LIT MS^n

m/z	Rel. Int.	Theo. Mass	Deviation	RDB equiv.	Composition	[a]structures			
Da	%	Da	mDa			subfamily	a	b	c
1122.1665	4.69	1122.1665	0.02	2.5	C76 H147 O3 Li2	α-MA	[b]		
1150.1977	81.16	1150.1978	-0.13	2.5	C78 H151 O3 Li2	α-MA	20	14	11
1164.2135	4.2	1164.2134	0.09	2.5	C79 H153 O3 Li2	α-MA	[b]		
1178.2291	100	1178.2291	-0.03	2.5	C80 H155 O3 Li2	α-MA	20	14	13
1192.2451	3.43	1192.2447	0.39	2.5	C81 H157 O3 Li2	α-MA	[b]		
1206.2604	46.02	1206.2604	0	2.5	C82 H159 O3 Li2	α-MA	20	14	15
							20	16	13
1234.2920	19.76	1234.2917	0.28	2.5	C84 H163 O3 Li2	α-MA	20	14	17
1238.2868	12.27	1238.2866	0.19	1.5	C83 H163 O4 Li2	methoxy	18	14	17
							18	16	15
1250.2871	11.94	1250.2866	0.49	2.5	C84 H163 O4 Li2	keto	18	18	15
							16	18	17
1264.3026	3.91	1264.3022	0.34	2.5	C85 H165 O4 Li2	keto	16	19	17
1266.3179	68.88	1266.3179	0.01	1.5	C85 H167 O4 Li2	methoxy	18	16	17
1278.3177	54.8	1278.3179	-0.19	2.5	C86 H167 O4 Li2	keto	18	18	17
							20	18	15
1292.3332	37.52	1292.3335	-0.33	2.5	C87 H169 O4 Li2	keto	18	19	17
1294.3505	45.12	1294.3492	1.29	1.5	C87 H171 O4 Li2	methoxy	18	18	17
1306.3492	3.07	1306.3492	-0.04	2.5	C88 H171 O4 Li2	keto	[b]		
1308.3655	7.1	1308.3648	0.66	1.5	C88 H173 O4 Li2	methoxy	18	19	17
1320.3649	4.09	1320.3648	0.07	2.5	C89 H173 O4 Li2	keto	[b]		
1322.3808	9.33	1322.3805	0.33	1.5	C89 H175 O4 Li2	methoxy	18	18	19

[a]The minor isomers with C22-α-alkyl chain are not defined. [b]Structure not determined.

https://doi.org/10.1021/jasms.1c00310
J. Am. Soc. Mass Spectrom. 2022, 33, 149−159

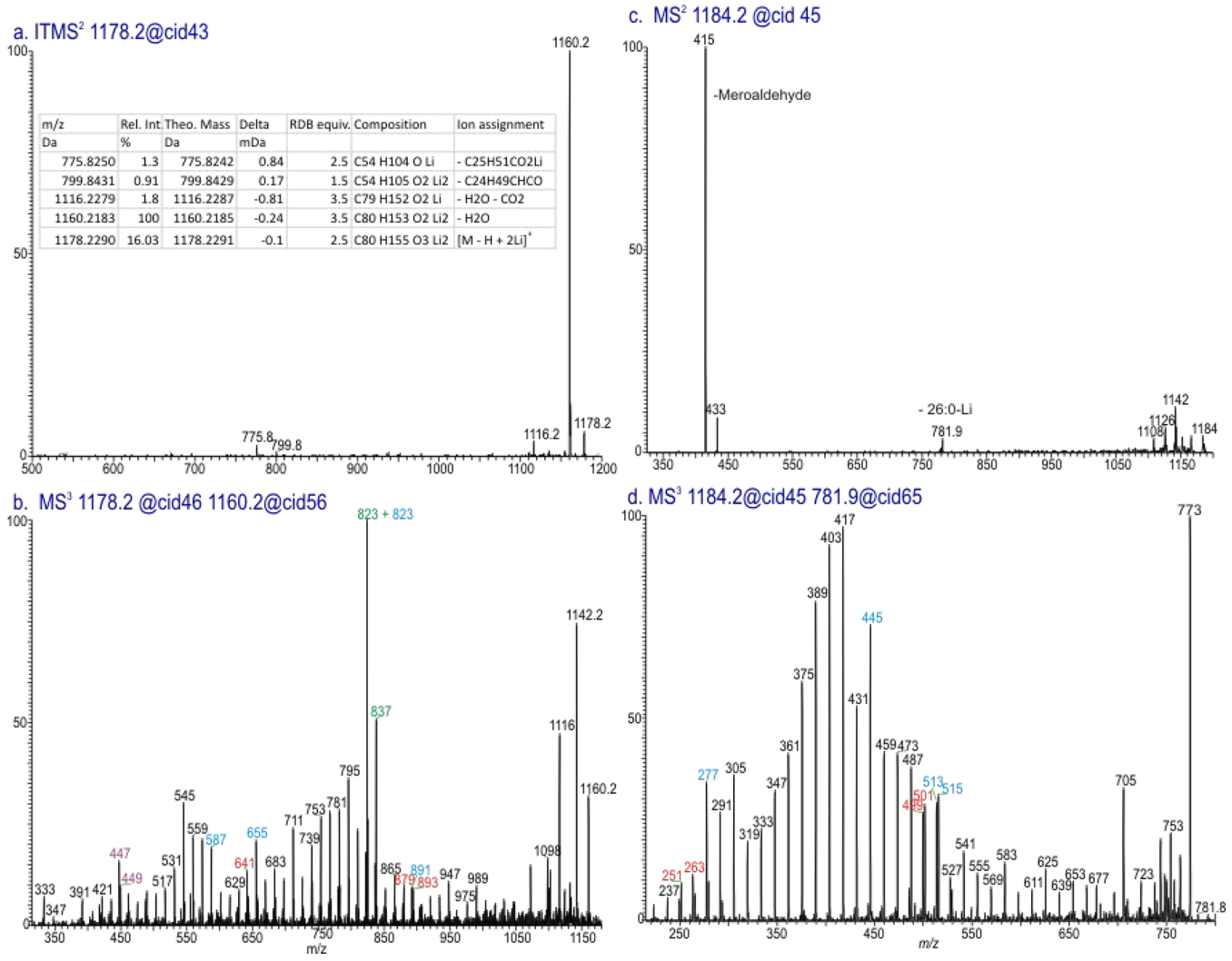

Figure 1. (a) The MS^2 spectrum of the $[M - H + 2Li]^+$ ion of C54:2(20,14,13)/C26:0-αMA at m/z 1178, (b) its MS^3 spectrum of the ion of m/z 1160 (1178 → 1160), (c) the MS^2 spectrum of the $[M - 2H + 3Li]^+$ ion of m/z 1184, and (d) its MS^3 on the ion of m/z 782 (1184 → 782). The inset in panel a shows the HRMS that supports the ion assignments. Please note: due to the mass defect, some of the nominal mass (m/z) labeling may have a −1 Da deviation from the accurate m/z.

$H]^-$ ions of MA yield mainly a α-branched long chain fatty acid anion by β-cleavage to eliminate meroaldehyde chain.[29] For example, the CID MS^2 spectra of the ion of m/z 1136 (Figure s2a) in the α-mycolic acid subfamily of the ion of m/z 1252 (Figure s2b) in the methoxy MA family and of the ion of m/z 1264 (not shown) in the keto MA family (Table 1) are all dominated by the ion of m/z 395 representing a hexacosanoic acid (26:0) anion, indicating that the molecules consist of an α-C24:0-alkyl chain. Although the chain length of the meroaldehyde chain can thus be deduced, the detailed structure information, for example, the location of the functional groups such as the cyclopropane ring, methoxy, and keto groups along the meroaldehyde chain, is unavailable. Thus, while characterization of MA as $[M - H]^-$ ions using MS^2 provides good sensitivity and useful information to identify the α-alkyl chain, the LIT MS^n on the $[M - H]^-$ ion for complete structural characterization is not feasible.[29]

Structural Characterization of MA as Lithiated Adduct Ions. When subjected to ESI in the positive ion mode in the presence of Li^+ (to avoid isotope distribution, we used monoisotopic ^{7}LiOH as Li^+ source), MA formed $[M + Li]^+$, $[M + 2Li - H]^+$ and $[M + 3Li - 2H]^+$ ions depending on the concentration of Li^+ with significantly lower sensitivity than that seen as the $[M - H]^-$ ion in the negative ion mode. For example, in the presence of 2 nM methanolic ^{7}LiOH (with 50 pmol/μL of mycolic acid), ions in the form of $[M + 2Li - H]^+$ are the dominant species (Figure s1b). The ESI LIT MS^n approaches toward the underlining fragmentation mechanisms that led to characterize the *Mtb* mycolic acids as the lithiated species are described below.

The LIT MS^n Mass Spectra of the Synthetic Mycolic Acid Standards. In order to gain insight into the fragmentation process of MAs, we acquired the LIT MS^n spectra on the mono- or dilithiated mycolic acid standards including C54:2(20,14,13)/C26:0-αMA, corynmycolic acid (C16:0/C16:0-MA), C56:1(18,16,17)/C26:0-mMA, and C58:2(20,18,15)/C26:0-kMA, which contain the specified α-alkyl chain, and various functional groups including cyclopropyl, methyl, methoxy, and keto groups along the meroaldehyde chain.

A. C54:2(20,14,13)/C26:0- αMA. We obtained the MS^2 spectrum of the $[M - H + 2Li]^+$ ion of C54:2(20,14,13)/C26:0- αMA at m/z 1178 (Figure 1a), which is dominated by the ion of m/z 1160 arising from loss of H_2O along with ion of

https://doi.org/10.1021/jasms.1c00310
J. Am. Soc. Mass Spectrom. 2022, 33, 149−159

Scheme 2. Fragmentation processes proposed for (a) the $[M - H + 2Li]^+$ and (b) the $[M - 2H + 3Li]^+$ Ions of C54:2(20,14,13)/26:0-αMA That Define the Structure of the Molecule

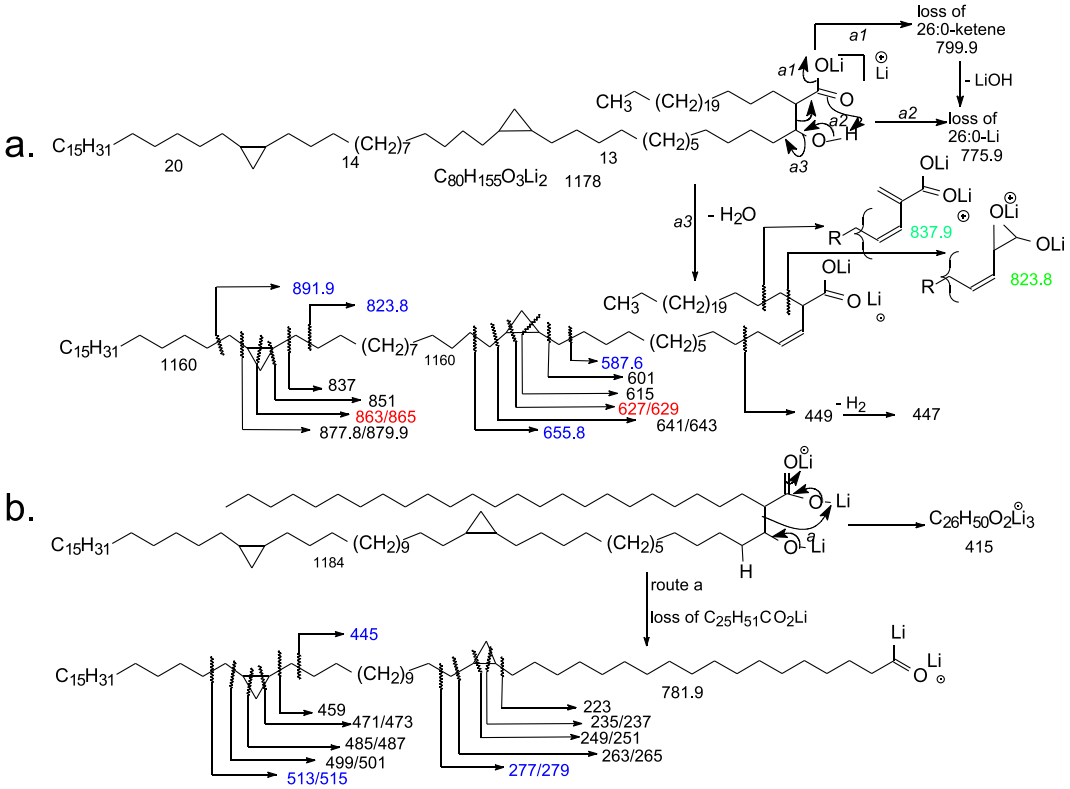

m/z 1116 arising from further loss of CO_2, and ions of m/z 799.9 and 775.9 arising from loss of 26:0-FA as a ketene (Scheme 2a, route *a1*) and as lithium salt (Scheme 2a, route *a2*), respectively. The formation of these ions is supported by high-resolution mass measurements (inset table, panel a). The presence of the ions of m/z 799 and 775 from loss of alkyl chain affords identification of the 24:0 α-alkyl chain of the molecule. Further dissociation of m/z 1160 (1178 → 1160, Figure 2b) yielded ions of m/z 447/449, 823, and 837, likely arising from allylic cleavages of the double bond (Scheme 2) formed by the H_2O loss via elimination of the β−OH and the γ-H (Scheme 2a, route *a3*). These fragmentation processes are further supported by the MS^n spectra of the $[M - H + 2Li]^+$ ion of C16:0/C16:0-MA (Figure s3), a short chain MA with no functional group on the meroaldehyde chain, in which the MS^3 spectrum of m/z 491 (509 → 491) (Figure s3, panel b) contained the abundant ions of 307/309, which is analogous to m/z 447/449 (a mass shift of 140 Da ($C_{10}H_{20}$)), and m/z 295, which is analogous to m/z 823 (a mass shift of 528 Da ($C_{10}H_{20}$ + $C_{28}H_{52}$)) (see inset in panel a for fragmentations). The observation of these ions is consistent with the identity of the α-alkyl chain.

The spectrum (Figure 1b) also contains ions of m/z 891, 877/879, 863/865, 851, 837, and 823 (same m/z as that from allylic cleavage), arising from cleavages of the C−C bonds of the distal cyclopropyl group, indicating the presence of ω21,22-methylene (cyclopropyl) group (i.e., a = 20), together with the ions of m/z 655, 641/643, 627/629, 615, 601, and 587, likely arising from similar cleavages of the proximal cyclopropane ring, indicating the presence of ω37,38-methylene (i.e., c = 13) group on the meroaldehyde chain.[16]

To further define the cyclopropyl chain, we also obtained the MS^2 spectrum of the $[M - 2H + 3Li]^+$ ion of m/z 1184 (Figure 1c), which contained the major ion of m/z 415 ($C_{26}H_{50}O_2Li_3^+$) arising from loss of meroaldehyde, and ion of m/z 781.9, arising from loss of 26:0-FA as lithium salt (loss of $C_{25}H_{51}CO_2Li$), consistent with the presence of 24:0 α-alkyl chain. MS^3 on the ion of m/z 781.9 (1184 → 781.9; Figure 2d) gave rise to ions of m/z 515/513, 501/499. 459, and 445, arising from cleavages of the distal cyclopropyl ring, and ions of m/z 279/277 and 265/263, arising from cleavages of the proximal cyclopropyl ring.[16] The structural information points to the location of the cyclopropane rings on the meroaldehyde chain.

B. C59:1(18,16,17)/26:0-mMA. By contrast, the MS^2 spectrum of the $[M - H + 2Li]^+$ ion of C59:1(18,16,17)/26:0-mMA at m/z 1266 (Figure 2a) is dominated by the ions of m/z 887.9, 869.9, and 863.9 arising from loss of 26:0-FA as a ketene, an acid, and a lithium salt, respectively. These cleavages of 24:0 α-alkyl chain to eliminate 26:0-FA in various forms are also supported by high-resolution mass measurements (Supporting Information Table s1) and readily defined the 24:0-α-alky chain.

Further dissociation of the ion of m/z 869.9 (1266 → 869) gave rise to the major ion of m/z 837.9 (data not shown) arising from loss of CH_3OH. This CH_3OH loss is also supported by high-resolution mass measurement (Table s2), and the losses likely arise from cleavages of the methoxy group and the adjacent α (or α′)-hydrogens to form both a ω^{19} (or n-19) (Scheme 3a) and a ω^{20} (or n-20) alkenes (Scheme 3b). These fragmentation processes are further supported by the MS^4 spectrum of the ion of m/z 837.8 (1266 → 869.9 → 837.8; Figure 2b), which contains ions of m/z 599 (loss of

https://doi.org/10.1021/jasms.1c00310
J. Am. Soc. Mass Spectrom. 2022, 33, 149−159

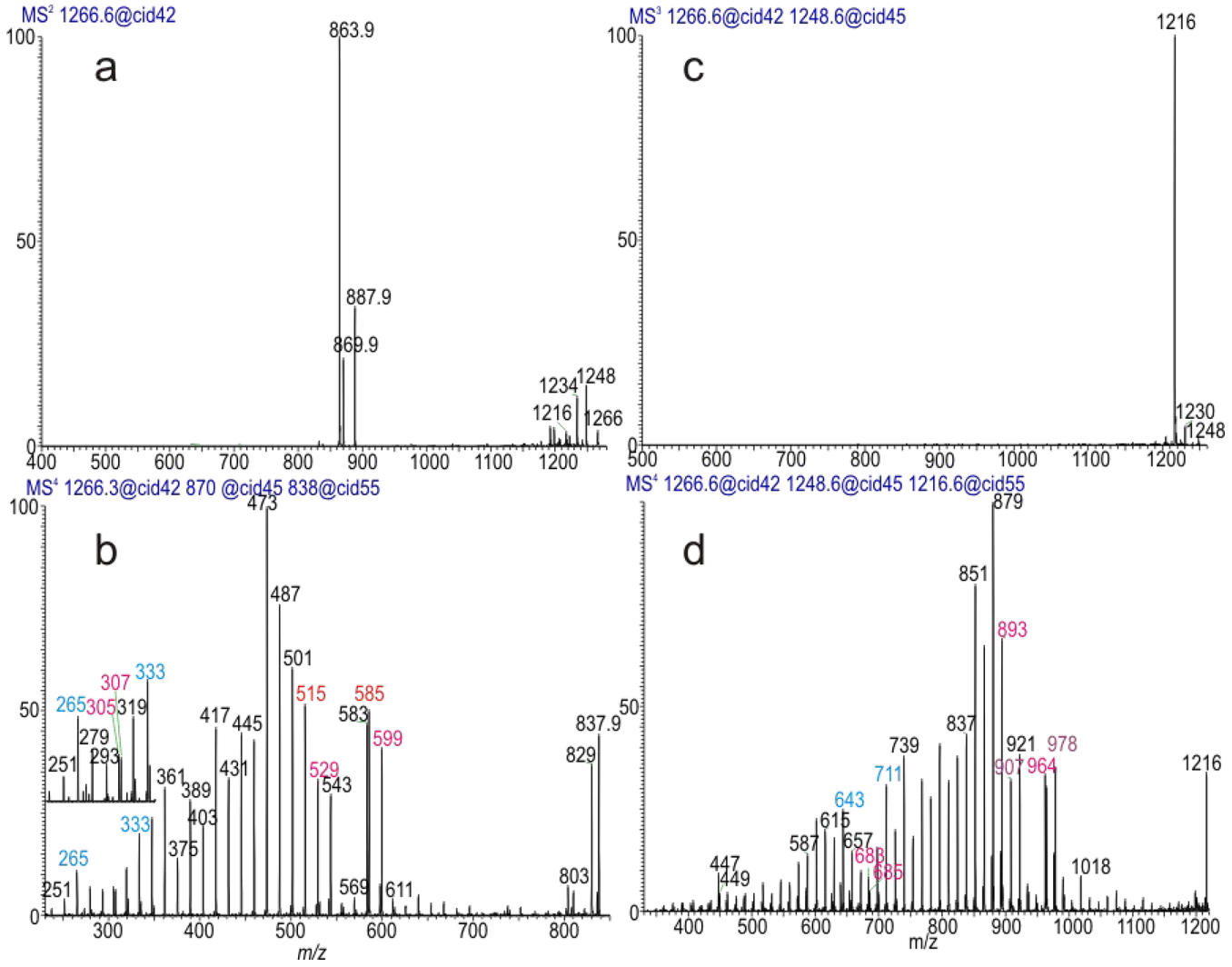

Figure 2. (a). The MS^2 spectrum of the $[M - H + 2Li]^+$ ion of C59:1(18,16,17)/26:0-mMA at m/z 1266, (b) its MS^4 spectrum of the ion of m/z 838 (1266 → 870 → 838), (c) its MS^3 spectrum of the ion of m/z 1248 (1266 → 1248), and (d) MS^4 spectrum of the ion of m/z 1216 (1266 → 1248 → 1216).

$CH_3(CH_2)_{14}CH{=}CH_2$) and 529 (loss of $CH_3(CH_2)_{17}CH(CH_3)CH{=}CH_2$) by allylic cleavage of the ω^{19} double bond on the meroaldehyde chain, respectively,[30] together with ions of m/z 585 and 515, arising from similar allylic cleavage of the ω^{20} double bond. The structural information readily locates the methoxy and methyl groups on the meroaldehyde chain. The spectrum (Figure 2b) also contained the ions at m/z 333, 319/321, 305/307, 293, 279 and 265, indicating the presence of ω-37,38 methylene (cyclopropyl),[31] consistent with the notion that the cyclopropyl ring is situated at ω-37.

In Figure 2a, an ion at m/z 1248, arising from the similar loss of H_2O involving the participation of the β−OH group and the adjacent hydrogens to form a double bond is also present. Further dissociation of the ion of m/z 1248 (1266 → 1248, Figure 2c) gave rise to m/z 1216 by loss of CH_3OH to form a double bond via elimination of the methoxy group and the adjacent hydrogen as seen earlier (Scheme 4 a,b). The MS^4 spectrum of the ion of m/z 1216 (1266 → 1248 → 1216, Figure 2d) contained the ions at m/z 447/449, and 879.9 arising from allylic cleavage of the double bond arising from the water loss similar to those seen for αMA (Scheme 1a) (Scheme 3a,b), along with ions of m/z 977.9/907.9 arising from allylic cleavage of the double bond at ω-19 (formed by loss of the methoxy group and the adjacent secondary hydrogen) (Scheme 3a), and the ions of m/z 963.9/893.9 arising from allylic cleavage of the double bond at ω-20 (Scheme 3b). The observation of these ions affords locating the methoxy and methyl side chains of the molecule. The spectrum also contained the ions at m/z 711, 697/699, 683/685, 671, 657, and 643, indicating the presence of the ω-37,38 methylene (cyclopropyl) (i.e, b = 16), pointing to that the c-segment is 17 (i.e., c = 17) (Scheme 4).

C. C60:2(20,18,15)/C26:0- kMA. The MS^2 spectrum of C60:2(20,18,15)/C26:0- kMA at m/z 1278 (Figure 3a) contained major ions of m/z 899.9, 881.9, and 875.9, arising from loss of hexacosanoic acid (26:0) as a ketene (loss of 378 Da), an acid (loss of 396 Da), and a lithium salt (loss of 402 Da), respectively, indicating the presence of an α-24:0-alkyl side chain, as seen earlier. Further elimination of LiOH from the ion of m/z 899.9 yielded ions of m/z 875.9, which gave rise to ions at m/z 607, 595/593, 567, 539/537, and 523 arising from cleavages of $CH_2(40)$−$CH(39)$, $CH(39)$−$CH(38)CH_3$, $CH(38)CH_3$−$C(37)O$, $C(37)O$−$CH_2(36)$, and $CH_2(36)$−$CH_2(35)$ bonds of the meroaldehyde chain, respectively (1278

https://doi.org/10.1021/jasms.1c00310
J. Am. Soc. Mass Spectrom. 2022, 33, 149−159

Scheme 3. Fragmentation Processes Proposed for the [M − H + 2Li] + Ions of C59:1(18,16,17)/26:0-mMA at m/z 1266.3 That Undergo Fragmentations via MS^3 (1266 → 869) and MS^4 (1266 → 869 → 837) Routes for Structure Characterization

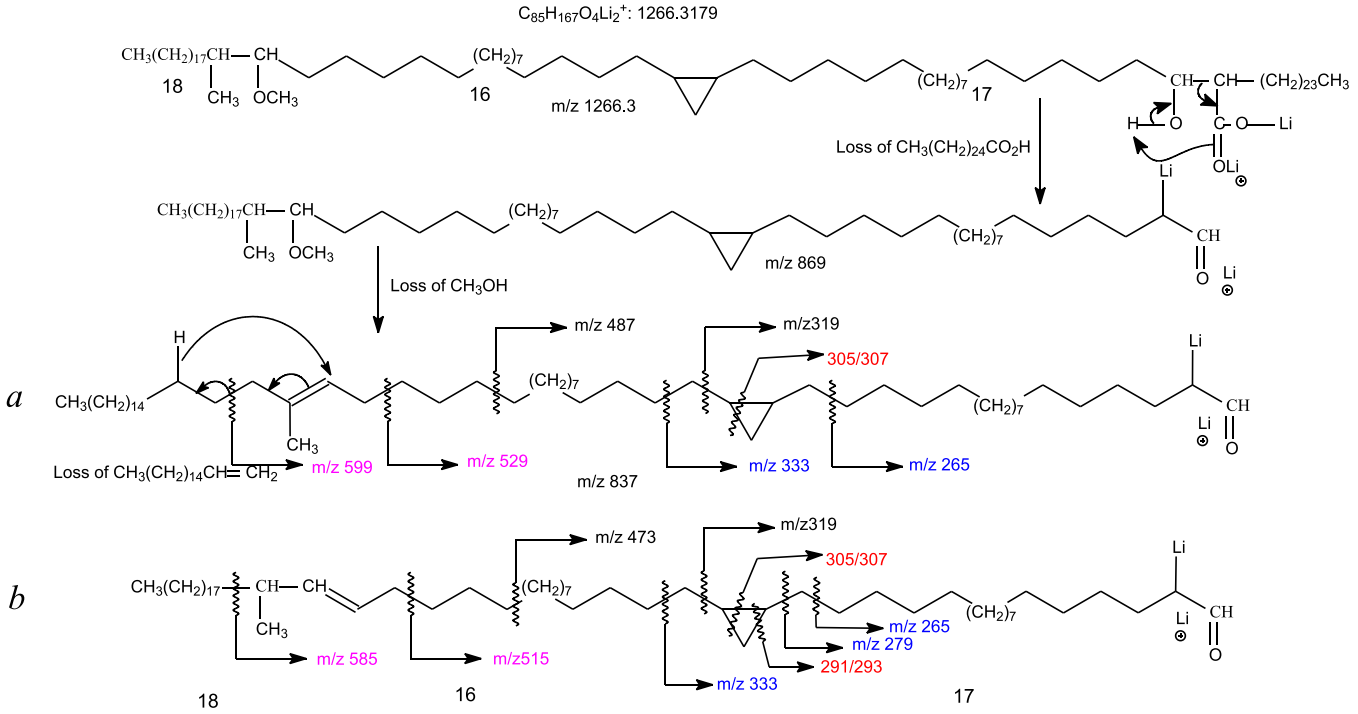

Scheme 4. Fragmentation Processes Proposed for the [M − H + 2Li]+ Ions of C59:1(18,16,17)/26:0-mMA at m/z 1266.3 that Undergo Fragmentations via MS^3 (1266 → 1248) and MS^4 (1266 → 1248 → 1216) Routes for Structure Characterization

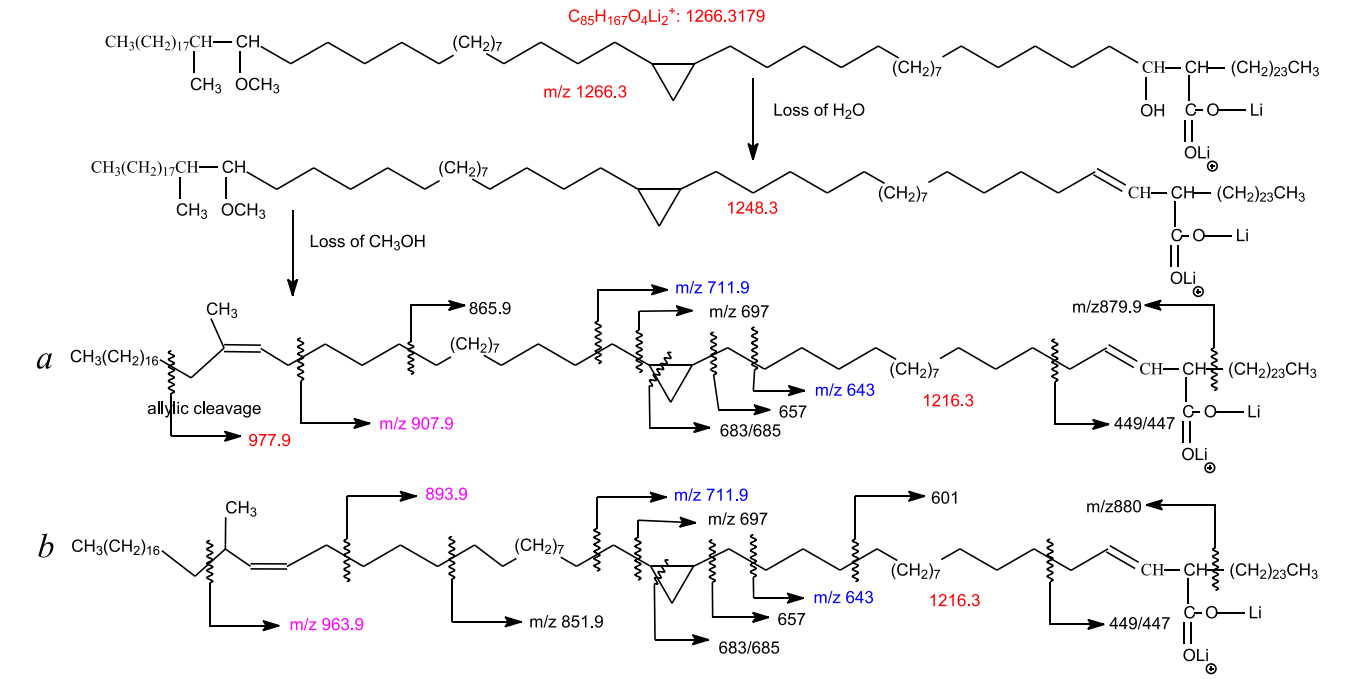

→ 875.9; Figure 3b). The results are consistent with the location of the methyl side chain, and the carbonyl group on the meroaldehyde (Scheme 5).

The ion of *m/z* 881.9 in Figure 3a is a dilithiated meroaldehyde, which gave rise to the analogous ions of *m/z* 613, 601/599, 573, 545/543, and 529 (Figure 3c) (MS^3 (1278 → 882)) that are 6 Da (the difference of Li and H) heavier than the ions of *m/z* 607, 595/593, 567, 539/537, and 523 seen for *m/z* 875.9 (Figure 3b). The results are in accord with the fragmentation processes and lead to locating the CO functional group and the methyl side chain (Scheme 5). The spectrum (Figure 3c) also contained the abundant ion at *m/z* 873.9, arising from loss of LiH. Further dissociation of ion of *m/z* 873.9 (1278 → 881.9 → 873.9) (not shown) gave rise to the analogous ions of *m/z* 605, 593/591, 565, 537/535 and 521 that are 8 Da (LiH) lighter than those seen in Figure 3c.

https://doi.org/10.1021/jasms.1c00310
J. Am. Soc. Mass Spectrom. 2022, 33, 149−159

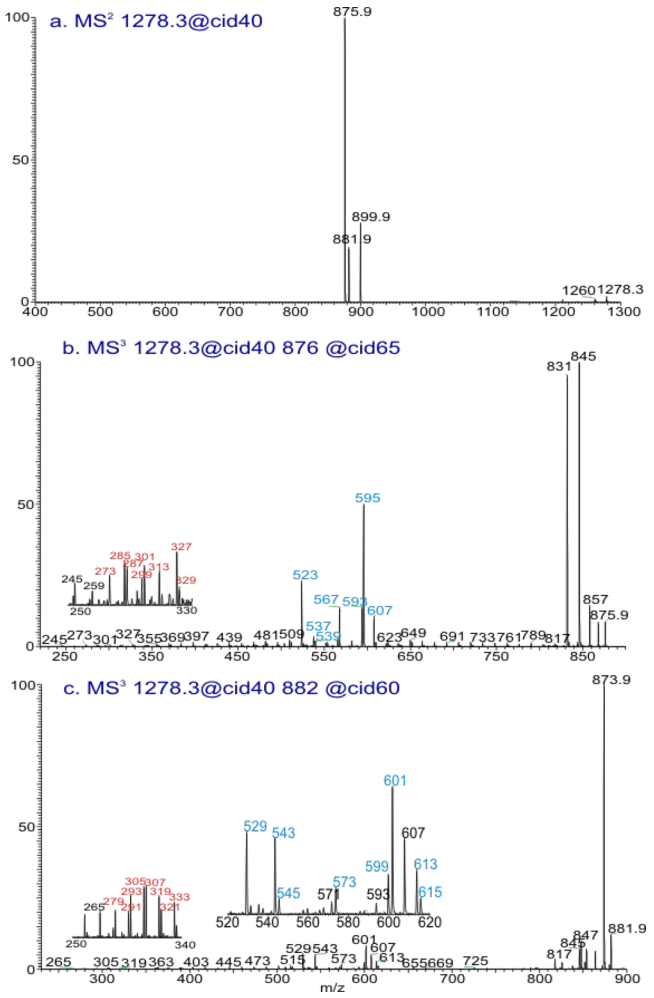

Figure 3. (a) The MS^2 spectrum of the $[M - H + 2Li]^+$ ion of C60:2(20,18,15)/C26:0- kMA at m/z 1278, (b) its MS^3 spectra of the ion of m/z 876 (1278 → 876; Figure 4b), and (c) of m/z 882 (1278 → 882).

The results again, are in agreement with the proposed fragmentation processes.

We speculate that the ions at m/z 327/329, 313, 299/301, 285/287 in Figure 3a and ions at 333/335, 319, 305/307. 291/293 in Figure 3b (insets, where the m/z values are marked in red) are related to the cleavages of the cyclopropane ring. These ions are of low abundance and the location of the cyclopropane ring cannot be unambiguously defined.

We then explored the utility of LIT MS^n on the $[M + Li]^+$ ions of kMA in the structural characterization. As shown in Figure 4a, the MS^2 spectrum of the $[M + Li]^+$ ions at m/z 1272

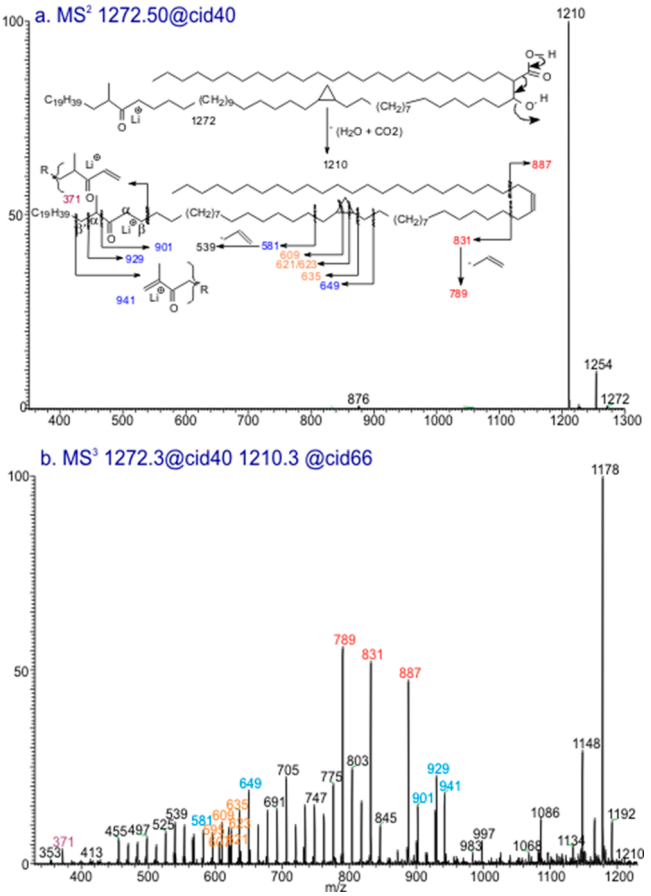

Figure 4. (a) The MS^2 spectrum of the $[M + Li]^+$ ions C60:2(20,18,15)/C26:0- kMA at m/z 1272, and (b) its MS^3 spectrum of the ion of m/z 1210 (1272 → 1210). The inset in panel a shows the proposed fragmentation pathways leading to the structural assignment.

is dominated by the ions of m/z 1210, arising from losses of H_2O and CO_2 by cleavage of the β−OH group and the carboxylate to form a double bond (see Figure 4a, inset for fragmentations). The ion of m/z 1210 is a monolithiated cation in which the Li^+ is likely situated at the carbonyl group of meroaldehyde. This speculation is based on the findings that the MS^3 spectrum of the ion of m/z 1210 (1272 → 1210;

Scheme 5. Fragmentation Processes Proposed for C60:2(20,18,15)26:0-kMA

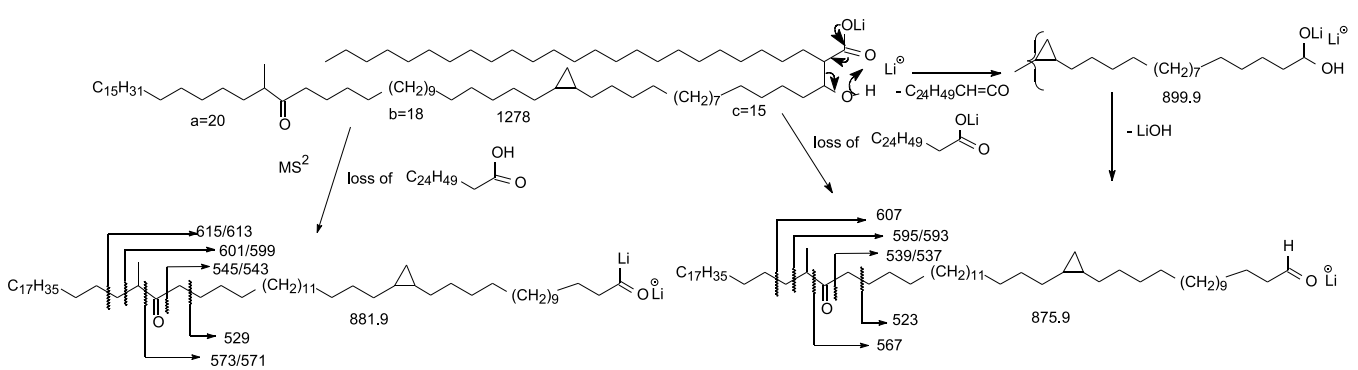

https://doi.org/10.1021/jasms.1c00310
J. Am. Soc. Mass Spectrom. 2022, 33, 149−159

Figure 4b) contained the ions of m/z 929.9 and 901.9 likely arising from cleavage of ω-end C20−21, and C21−C22 bond, respectively, along with ions of m/z 941.9 (β') and 371 (β) arising from β-cleavage of C−C bond of the carbonyl group (Figure 4a, inset scheme).[16] The presence of these ions provides information to locate the keto and the methyl groups. More importantly, the spectrum contained the ions of m/z 649, 635, 621/623, 609/607, and 595 that revealed the 21,22-methylene (cyclopropyl) chain, whereas the ions of m/z 887.9 and 831.9 may arise from allylic cleavages of the double bond formed by (H_2O + CO_2) loss upon CID MS^2 on the $[M + Li]^+$ ion of m/z 1272 to 1210.

Characterization of *Mtb* Mycolic Acids. We next applied the same LIT MS^n approaches to reveal the structures of *Mtb* MA. High-resolution ESI-MS (Figure s1a and b) easily segregates α-, methoxy-, and keto-mycolic acids due to their distinguishable elemental compositions. For example, in the negative ion mode, the $[M - H]^-$ ions of α-, methoxy-, and keto-mycolic acids possess a $C_nH_{2n-5}O_3$, $C_nH_{2n-3}O_4$, and $C_nH_{2n-5}O_4$,(where n = 76 to 90) elemental composition, respectively, with double bond (RDB) equivalents of 3.5, 2.5, and 3.5 (the surplus one-half double bond is due to the negative charge on the ion), respectively (Table s1). This is consistent with the observation of the corresponding ions with $C_nH_{2n-6}O_3Li_2$, $C_nH_{2n-4}O_4Li_2$, and $C_nH_{2n-6}O_4$ Li_2, (where n = 76 to 90) elemental composition for α-, methoxy-, and keto-mycolic acids, respectively, in the positive ion mode (Table 1). The mass spectrometric approaches applying LIT MS^n on the $[M - H + 2Li]^+$ ions toward structural identification of Mtb mycolic acids are described below.

***α*-Mycolic Acids.** The majors ions in the α-mycolic acid family desorbed as the $[M - H + 2Li]^+$ ions in the positive ion mode were seen at m/z 1122, 1150, 1164, 1178, 1192, and 1206 which possess two cyclopropyl rings. The LIT MS^2 spectrum of the ion of m/z 1178, and MS^3 spectrum of the ion of m/z 1160 (1178 → 1160) are identical to the synthetic standard (Figure 1), pointing to the assignment of C54:2-(20,14,13)/C26:0-αMA structure. Similarly, the MS^2 spectrum of the ion of 1150 (data not shown) is dominated by the ion of m/z 1132 arising from loss of H_2O, along with ions of m/z 753.7 and 781.8 arising from loss of 26:0- and 24:0-FA, respectively, indicating the presence of the major α-24:0- and minor α-22:0-alkyl chains. The MS^3 spectrum of the ion of m/z 1132 (1150 → 1132; Figure 5a) contained ions analogous to those from the synthetic standard (Figure 2b), but the ions at m/z 865/863, 851, 835/837, and 809 arising from cleavages of the distal cyclopropyl ring, and the ions of m/z 627, 613/615, 599/601 arising from cleavages of the proximal cyclopropyl ring were 28 Da (C_2H_4) lighter, indicating that the methylene side chains are situated at ω21 (i.e., a = 20), and ω37 (i.e., b = 14; c = 11) (see inset scheme for fragmentation). The spectrum also contained the ions of m/z 447/449, consistent with the fragmentation process that forms m/z 1132 from m/z 1150 by loss of H_2O to form a double bond. The above structure information gives assignment of C52:2(20,14,11)/C26:0- αMA.

Similarly, the LIT MS^2 spectrum of the ion of m/z 1206 (data not shown) is dominated by the ion of m/z 1188, which yielded a MS^3 spectrum (1206 → 1188; Figure s4) containing ions of m/z 921.9/919.9, 907.9/905.9, 865.9, and 851.9, along with ions of m/z 683 and 615. These ions are 28 Da higher than the analogous ions seen for the standard C54:2-(20,14,13)/C26:0-αMA at m/z 1178 (Figure 1a), leading to the assignment of C56:2(20, 14, 15)/C26:0- αMA structure.

Methoxy Mycolic Acids. There are five major species seen at m/z 1238, 1266, 1294, 1308, and 1322. The MS^n spectra of the ion of m/z 1266 (data not shown) are identical to those obtained from the synthetic standard (Figure 2), leading to the assignment of C59:1(18,16,17)/26:0-mMA structure. Characterization of other species in this subfamily is exemplified by the ion of m/z 1294, which gave rise to a MS^2 spectrum containing major ions at m/z 915.9 (loss of 26:0-FA ketene), 897.9 (loss of 26:0-FA), and 891.9 (loss of 26:0-FA lithium salt) that identify the 24:0-α-alkyl chain (Figure s5a). The MS^3 spectrum of the ion of m/z 897.9 is dominated by the ion of m/z 865.9 (Figure s5b), which arose from loss of methanol by elimination of the methoxy side chain and adjacent hydrogen to form a double bond as described earlier. The MS^4 spectrum of the ion of m/z 865.9 (1294 → 897.9 → 865.9; Figure 5b) contained ions of 627/625, 557, together with ions of 611/613 and 533, indicating the location of the double bonds generated from methanol loss, and thus providing the location of the methoxy and methyl side chains (i.e., a = 18) (see Figure 4b, inset scheme for fragmentation). The spectrum also contained ions of m/z 333, 319/321, 305/307, 293, 279, and 265, which identify the ω-39,40 methylene (cyclopropyl) group (i.e., c = 17). Taken together, these results led to the assignment of C61:1(18,18,17)/26:0-mMA.

Keto Mycolic Acids. The most abundant species in this subfamily was seen at m/z 1278, which possesses an elemental composition identical to the synthetic standard. The MS^2 spectrum of the $[M - H + 2Li]^+$ ions at m/z 1278 (data not shown) is identical to that shown in Figure 3a, containing ions of m/z 899.9, 881.9 (loss of 26:0-FA), and 875.9 (loss of 26:0-FA lithium salt), indicating the presence of C24:0 α-alkyl chain. The MS^3 spectrum of m/z 875.9 (Figure 5c) contained ions of m/z 867.9 (loss of LiH) 857.9 (loss of H_2O), 845.8 (Loss of HCHO), 831.8 (loss of [CO_2 + H_2]) similar to those seen for k-MA standard (Figure 3b), together with ions of m/z 551, 595, 621/623, and 635, which are 28 Da (C_2H_4 chain) heavier than those seen in Figure 3b, indicating that the methyl side chain and keto group are located at ω-21 and ω-22, respectively (i.e., a = 18). The spectrum also contained the ions of m/z 355, 341/343, 327/329, 313/315, and 301, which are also 28 Da (C_2H_4 chain) heavier than those seen in Figure 3b. These mass shifts indicate that methylene (cyclopropyl) group is situated at ω39 (i.e., ω39,40 methylene). The combined information led to assign a C60:2(18,18,17)/C26:0-kMA structure.

In addition to the above ions that identify the major structure, the spectrum also contained the ion set of m/z 623, 595, 565, and 551 along with ions at m/z 343, 329/327, 315/313 that were seen for the synthetic C58:2(20,18,15)/C26:0-kMA standard (Figure 3c). The results indicate that a minor C60:2(20,18,15)/C26:0-kMA isomer identical to the synthetic standard is also present.

To confirm the above structure assignment, we obtained the MS^3 spectrum of the ion of m/z 1210 (1272 → 1210) (Figure 5d) from the corresponding $[M + Li]^+$ ions of m/z 1272. The spectrum contained the abundant ions of m/z 887, 821, and 779 arising from the similar β-cleavages of the double bond (Figure 4b; inset scheme), and the ion set of m/z 957, 929, 969.9 (β'), and 343 (β), driving from cleavages of C−C bonds containing the methyl and keto chain, together with ions of m/z 621, 607/609, 593/595, 553, and 511 arising from cleavages

https://doi.org/10.1021/jasms.1c00310
J. Am. Soc. Mass Spectrom. 2022, 33, 149−159

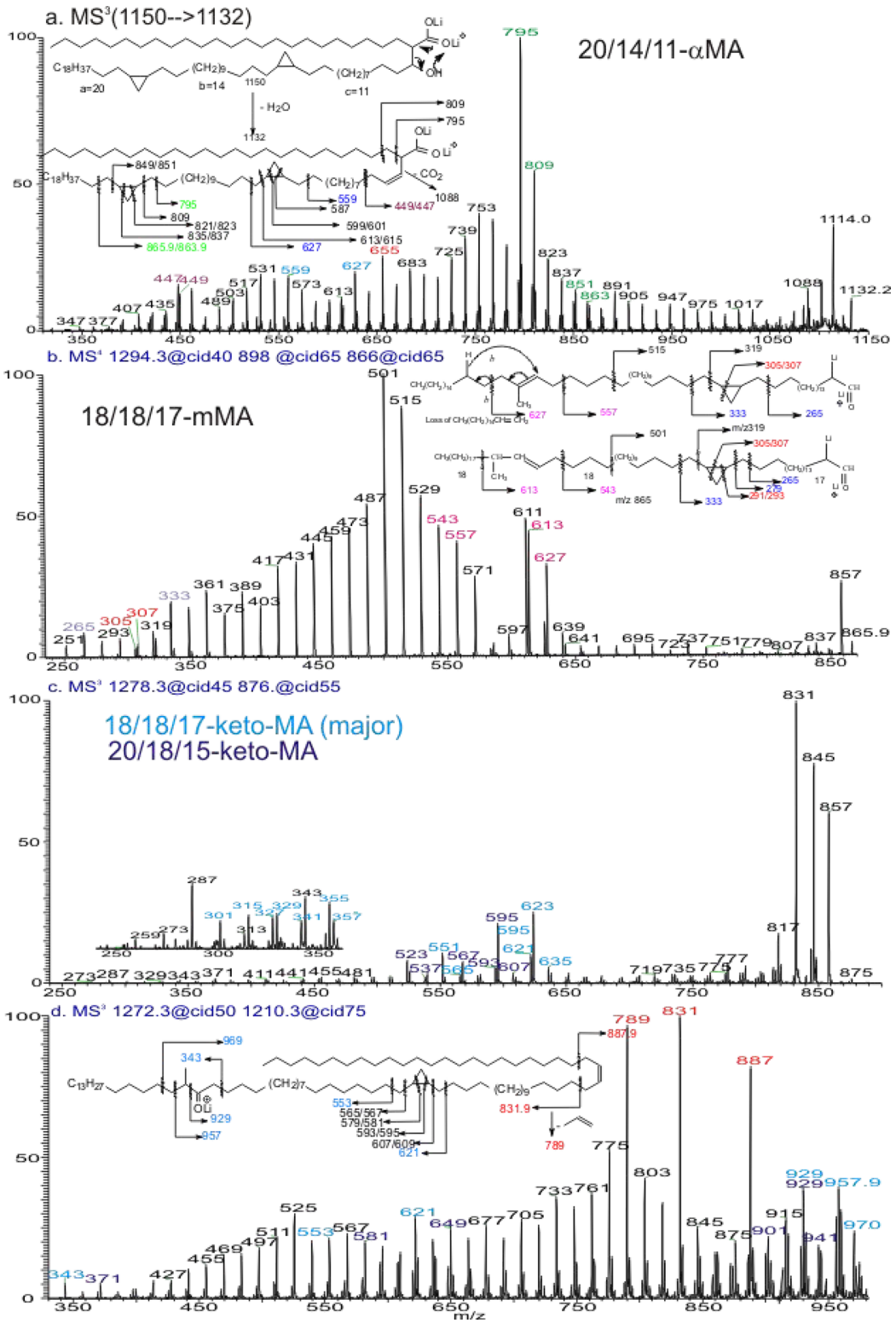

Figure 5. (a) The MS^3 spectrum of the ion of m/z 1132 (1150 → 1132) that led to assign C52:2(20,14,11)/C26:0-αM structure; (b) MS^4 spectrum of the ion of m/z 865.9 (1294 → 897.9 →865.9) that led to C61:1(18,18,17)/26:0-mMA. (c) MS^3 spectra of the ion of m/z 875.9 (1278 → 875.9) and (d) of ion of m/z 1210 (1272 → 1210) that led to identify C60:2(18,18,17)/C26:0- kMA structure. The mycolic acids are from *Mtb* (bovine strain), and each spectrum represents the three major mycolic acid subfamilies (α-, methoxy-, and keto) that contain various functional groups on the meroaldehyde chains. The MS^2 spectra of the $[M - H + 2Li]^+$ ions (i.e., m/z 1150, m/z 1294, and of m/z 1278), and of the $[M + Li]^+$ ion (i.e., m/z 1272) for the MAs (data not shown) can only provide information on the α-alkyl (mainly C24-alkyl) chain. However, the LIT MS^n (n = 3,4) spectra readily permit complete determination of the mycolic acid structures in Mtb. Please note, in Panel d, only structurally informative ions in the mass range of m/z 330−980 are shown.

https://doi.org/10.1021/jasms.1c00310
J. Am. Soc. Mass Spectrom. 2022, 33, 149−159

of the cyclopropyl ring. These results readily afford defining the major C60:2(18,18,17)/C26:0- kMA structure. The spectrum also contained ion sets of 929, 901, 941.9 (β'), and 371 (β) and of m/z 649, 635/637, 621/623, 581 that were seen for the C60:2(20,18,15)/C26:0-kMA standard, consistent with the presence of a minor C60:2(20,18,15)/C26:0-kMA isomer as noted earlier.

Similarly, the MS^2 spectrum of the $[M - H + 2Li]^+$ ion of m/z 1292 in the kMA subfamily (Table 1) is dominated by the ions of 913.9 (loss of 26:0-ketene), 895.9 (loss of 26:0-FA), and 889.9 (loss of 26:0-FA lithium salt) (data not shown) signifying the presence of C24:0 α-alkyl chain. Further dissociation of the ion of m/z 889 (1292 → 889; Figure s6) gave rise to ions of m/z 649, 635/637, 609, and 565, which are 42 Da (C_3H_6) heavier than those seen for the synthetic C60:2(20,18,15)/C26:0- kMA standard (Figure 3), indicating that the methyl side chain and keto group are located at ω-21 and ω-22, respectively (i.e., a = 18). The spectrum also contained the ions of m/z 355, 341/343, 327/329, 313/315, and 301, which are identical to those seen for the synthetic standard (Figure 3b), indicating the presence of ω40,41 methylene group. These results led to the assignment of a major C61:2(18,19,17)/C26:0- kMA structure.

CONCLUSIONS

The insight fragmentation mechanism revealed by studying the various mycolic acid standards plus the precise elemental composition obtained by high-resolution mass spectrometry readily permits near complete definition of the entire Mtb mycolic acid structures, including the location of the methoxy, methyl, cyclopropyl functional groups and the α-alkyl chain (Table 1). The assigned structures are in agreement with those previously reported by Watanabe and co-workers, who utilized FAB ionization method and a four sector tandem mass spectrometer with array detector to determine various Mtb mycolic acids, which were first prepared to mycolic acid methyl esters, pyrolyzed to meromycolaldehydes, and oxidized to meromycolic acids, followed by high energy CID MS/MS analysis of the meromycolic anions ($[M - H]^-$) desorbed by FAB to locate the functional groups.[16] The approach requires laborious sample preparation steps and painstaking mass spectrometric operation (FAB-high energy CID tandem sector mass spectrometer is relatively more complicated to operate), nevertheless showcased the application of the conventional tandem mass spectrometry in the characterization of complex lipid structures. In contrast, our approach is relatively simpler and more straightforward (no derivatization steps are required) for structure identification.

While the keto, methyl, and methoxy groups on the meroaldehyde can be unambiguously located using the present approach, less clear is the definition of the cyclopropyl groups due to that ions informative for identification of the cyclopropane rings are of low abundance, likely attributable to the fact that high (keV) collision energy may be required for the cleavages.[16,32] By contrast, the UVPD-MS method described by Blevins and co-workers can precisely locate the cyclopropane rings but cannot locate the methyl, methoxy, and keto functional groups on the meroaldehyde chain.[18] Since ions informative for assignment of the functional groups are all from MS^3 or MS^4 scans, a sustained signal average is often required to obtain a reliable spectrum for confident assignment using the present method. There is also no stereoisomeric assignment (i.e., cis or trans form of cyclopropyl ring) of the structure, which is not applicable using any CID MS^n methods. This information, nevertheless, has been reported by Watanabe and co-workers[16,17] as well as by Uenishi and co-workers using NMR spectroscopy.

ASSOCIATED CONTENT

Supporting Information

The Supporting Information is available free of charge at https://pubs.acs.org/doi/10.1021/jasms.1c00310.

Additional figures and tables (PDF)

AUTHOR INFORMATION

Corresponding Author

Fong-Fu Hsu − *Mass Spectrometry Resource, Division of Endocrinology, Metabolism, and Lipid Research, Department of Medicine, Washington University School of Medicine, St. Louis, Missouri 63110, United States;* orcid.org/0000-0001-5368-0183; Email: fhsu@wustl.edu

Authors

Cheryl Frankfater − *Mass Spectrometry Resource, Division of Endocrinology, Metabolism, and Lipid Research, Department of Medicine, Washington University School of Medicine, St. Louis, Missouri 63110, United States*

Hideji Fujiwara − *Mass Spectrometry Resource, Division of Endocrinology, Metabolism, and Lipid Research, Department of Medicine, Washington University School of Medicine, St. Louis, Missouri 63110, United States*

Spencer J. Williams − *School of Chemistry and Bio21 Molecular Science and Biotechnology Institute, University of Melbourne, Melbourne, Victoria 3010, Australia;* orcid.org/0000-0001-6341-4364

Adriaan Minnaard − *Stratingh Institute for Chemistry, University of Groningen, 9747 AG, Groningen, The Netherlands;* orcid.org/0000-0002-5966-1300

Complete contact information is available at: https://pubs.acs.org/10.1021/jasms.1c00310

Author Contributions

C.F. and H.F. collected the data, S.J.W. and A.M. prepared the samples, F.F.H. conceived, designed, and performed the analysis and wrote the paper.

Funding

United States Public Health Service Grants: U.S. Public Health Service Grants R24GM136766, P30DK020579, and R21AI144658.

Notes

The authors declare no competing financial interest.

ACKNOWLEDGMENTS

This work was supported by NIH P30DK020579, P30DK056341, and P41GM103422 grants to the Mass Spectrometry Resource of Washington University. We are indebted to the anonymous reviewers for their insightful comments on the paper.

REFERENCES

(1) Barry, C. E.; Lee, R. E.; Mdluli, K.; Sampson, A. E.; Schroeder, B. G.; Slayden, R. A.; Yuan, Y. Mycolic acids: structure, biosynthesis and physiological functions. *Prog. Lipid Res.* **1998**, *37*, 143−179.

(2) Portevin, D.; De Sousa-D'Auria, C.; Houssin, C.; Grimaldi, C.; Chami, M.; Daffé, M.; Guilhot, C. A polyketide synthase catalyzes the

last condensation step of mycolic acid biosynthesis in mycobacteria and related organisms. *Proc. Natl. Acad. Sci. U. S. A.* **2004**, *101*, 314−9.
(3) Takayama, K.; Wang, C.; Besra, G. S. Pathway to synthesis and processing of mycolic acids in Mycobacterium tuberculosis. *Clin. Microbiol. Rev.* **2005**, *18*, 81−101.
(4) Marrakchi, H.; Lanéelle, M.-A.; Daffé, M. Mycolic Acids: Structures, Biosynthesis, and Beyond. *Chem. Biol.* **2014**, *21*, 67−85.
(5) Laval, F.; Laneelle, M. A.; Deon, C.; Monsarrat, B.; Daffe, M. Accurate molecular mass determination of mycolic acids by MALDI-TOF mass spectrometry. *Anal. Chem.* **2001**, *73*, 4537−44.
(6) Kaneda, K.; Imaizumi, S.; Mizuno, S.; Baba, T.; Tsukamura, M.; Yano, I. Structure and Molecular Species Composition of Three Homologous Series of α-Mycolic Acids from Mycobacterium spp. *Microbiology* **1988**, *134*, 2213−29.
(7) Lanéelle, M. A.; Eynard, N.; Spina, L.; Lemassu, A.; Laval, F.; Huc, E.; Etienne, G.; Marrakchi, H.; Daffé, M. Structural elucidation and genomic scrutiny of the C60-C100 mycolic acids of Segniliparus rotundus. *Microbiology* **2013**, *159*, 191−203.
(8) Hong, S.; Cheng, T. Y.; Layre, E.; Sweet, L.; Young, D. C.; Posey, J. E.; Butler, W. R.; Moody, D. B. Ultralong C100 mycolic acids support the assignment of Segniliparus as a new bacterial genus. *PLoS One* **2012**, *7*, e39017.
(9) Guerrant, G. O.; Lambert, M. A.; Moss, C. W. Gas-chromatographic analysis of mycolic acid cleavage products in mycobacteria. *J. Clin. Microbiol.* **1981**, *13*, 899−907.
(10) Luquin, M.; Ausina, V.; López Calahorra, F.; Belda, F.; García Barceló, M.; Celma, C.; Prats, G. Evaluation of practical chromatographic procedures for identification of clinical isolates of mycobacteria. *J. Clin. Microbiol.* **1991**, *29*, 120−30.
(11) Kusaka, T.; Mori, T. Pyrolysis Gas Chromatography-Mass Spectrometry of Mycobacterial Mycolic Acid Methyl Esters and Its Application to the Identification of Mycobacterium leprae. *Microbiology* **1986**, *132*, 3403−6.
(12) Savagnac, A.; Aurelle, H.; Casas, C.; Coudere, F.; Gavard, P.; Prome, D.; Prome, J. C. Structure determination of mycolic acids by using charge remote fragmentation. *Chem. Phys. Lipids* **1989**, *51*, 31−8.
(13) Song, S. H.; Park, K. U.; Lee, J. H.; Kim, E. C.; Kim, J. Q.; Song, J. Electrospray ionization-tandem mass spectrometry analysis of the mycolic acid profiles for the identification of common clinical isolates of mycobacterial species. *J. Microbiol. Methods* **2009**, *77*, 165−77.
(14) Teramoto, K.; Suga, M.; Sato, T.; Wada, T.; Yamamoto, A.; Fujiwara, N. Characterization of Mycolic Acids in Total Fatty Acid Methyl Ester Fractions from Mycobacterium Species by High Resolution MALDI-TOFMS. *Mass Spectrom.* **2015**, *4*, A0035−A.
(15) Teramoto, K.; Tamura, T.; Hanada, S.; Sato, T.; Kawasaki, H.; Suzuki, K.; Sato, H. Simple and rapid characterization of mycolic acids from Dietzia strains by using MALDI spiral-TOFMS with ultra high mass-resolving power. *J. Antibiot.* **2013**, *66*, 713−7.
(16) Watanabe, M.; Aoyagi, Y.; Mitome, H.; Fujita, T.; Naoki, H.; Ridell, M.; Minnikin, D. E. Location of functional groups in mycobacterial meromycolate chains; the recognition of new structural principles in mycolic acids. *Microbiology* **2002**, *148*, 1881−902.
(17) Watanabe, M.; Aoyagi, Y.; Ridell, M.; Minnikin, D. E. Separation and characterization of individual mycolic acids in representative mycobacteria. *Microbiology* **2001**, *147*, 1825−37.
(18) Blevins, M. S.; Klein, D. R.; Brodbelt, J. S. Localization of Cyclopropane Modifications in Bacterial Lipids via 213 nm Ultraviolet Photodissociation Mass Spectrometry. *Anal. Chem.* **2019**, *91*, 6820−8.
(19) Uenishi, Y.; Fujita, Y.; Kusunose, N.; Yano, I.; Sunagawa, M. Comprehensive analysis of mycolic acid subclasses and molecular species composition of mycobacterium bovis BCG Tokyo 172 cell wall skeleton (SMP-105). *J. Microbiol. Methods* **2008**, *72*, 149−56.
(20) Hsu, F.-F.; Turk, J. Elucidation of the double-bond position of long-chain unsaturated fatty acids by multiple-stage linear ion-trap mass spectrometry with electrospray ionization. *J. Am. Soc. Mass Spectrom.* **2008**, *19*, 1673−80.
(21) Purdy, G. E.; Hsu, F.-F. Complete Characterization of Polyacyltrehaloses from Mycobacterium tuberculosis H37Rv Biofilm Cultures by Multiple-Stage Linear Ion-Trap Mass Spectrometry Reveals a New Tetraacyltrehalose Family. *Biochemistry* **2021**, *60*, 381−97.
(22) Flentie, K. N.; Stallings, C. L.; Turk, J.; Minnaard, A. J.; Hsu, F. F. Characterization of phthiocerol and phthiodiolone dimycocerosate esters of M. tuberculosis by multiple-stage linear ion-trap MS. *J. Lipid Res.* **2016**, *57*, 142−55.
(23) Hsu, F.-F. Characterization of Hydroxyphthioceranoic and Phthioceranoic Acids by Charge-Switch Derivatization and CID Tandem Mass Spectrometry. *J. Am. Soc. Mass Spectrom.* **2016**, *27*, 622−32.
(24) Rhoades, E. R.; Streeter, C.; Turk, J.; Hsu, F.-F. Characterization of Sulfolipids of Mycobacterium tuberculosis H37Rv by Multiple-Stage Linear Ion-Trap High-Resolution Mass Spectrometry with Electrospray Ionization Reveals That the Family of Sulfolipid II Predominates. *Biochemistry* **2011**, *50*, 9135−47.
(25) Hsu, F. F.; Turk, J.; Owens, R. M.; Rhoades, E. R.; Russell, D. G. Structural Characterization of Phosphatidyl-myo-Inositol Mannosides from Mycobacterium bovis Bacillus Calmette Guerin by Multiple-Stage Quadrupole Ion-Trap Mass Spectrometry with Electrospray Ionization. II. Monoacyl- and Diacyl-PIMs. *J. Am. Soc. Mass Spectrom.* **2007**, *18*, 479−92.
(26) Hsu, F. F.; Turk, J.; Owens, R. M.; Rhoades, E. R.; Russell, D. G. Structural characterization of phosphatidyl-myo-inositol mannosides from Mycobacterium bovis Bacillus Calmette Guerin by multiple-stage quadrupole ion-trap mass spectrometry with electrospray ionization. I. PIMs and lyso-PIMs. *J. Am. Soc. Mass Spectrom.* **2007**, *18*, 466−78.
(27) van der Peet, P. L.; Gunawan, C.; Torigoe, S.; Yamasaki, S.; Williams, S. J. Corynomycolic acid-containing glycolipids signal through the pattern recognition receptor Mincle. *Chem. Commun. (Cambridge, U. K.)* **2015**, *51*, 5100−3.
(28) Tahiri, N.; Fodran, P.; Jayaraman, D.; Buter, J.; Witte, M. D.; Ocampo, T. A.; Moody, D. B.; Van Rhijn, I.; Minnaard, A. J. Total Synthesis of a Mycolic Acid from Mycobacterium tuberculosis. *Angew. Chem., Int. Ed.* **2020**, *59*, 7555−60.
(29) Hsu, F.-F.; Soehl, K.; Turk, J.; Haas, A. Characterization of mycolic acids from the pathogen Rhodococcus equi by tandem mass spectrometry with electrospray ionization. *Anal. Biochem.* **2011**, *409*, 112−22.
(30) Hsu, F.-F.; Turk, J. Distinction among isomeric unsaturated fatty acids as lithiated adducts by electrospray ionization mass spectrometry using low energy collisionally activated dissociation on a triple stage quadrupole instrument. *J. Am. Soc. Mass Spectrom.* **1999**, *10*, 600−12.
(31) Hsu, F.-F.; Matthew Kuhlmann, F.; Turk, J.; Beverley, S. M. Multiple-stage linear ion-trap with high resolution mass spectrometry towards complete structural characterization of phosphatidylethanolamines containing cyclopropane fatty acyl chain in Leishmania infantum. *J. Mass Spectrom.* **2014**, *49*, 201−9.
(32) Frankfater, C.; Jiang, X.; Hsu, F. F. Characterization of Long-Chain Fatty Acid as N-(4-Aminomethylphenyl) Pyridinium Derivative by MALDI LIFT-TOF/TOF Mass Spectrometry. *J. Am. Soc. Mass Spectrom.* **2018**, *29*, 1688−99.

https://doi.org/10.1021/jasms.1c00310
J. Am. Soc. Mass Spectrom. 2022, 33, 149−159